

## MODELING OF GAS PARAMETERS IN THE CYLINDER OF THE AUTOMATIC GUN DURING FIRING

by

**Dejan T. JEVTIĆ<sup>a\*</sup>, Dejan M. MICKOVIĆ<sup>a</sup>, Slobodan S. JARAMAZ<sup>a</sup>,  
Predrag M. ELEK<sup>a</sup>, Miloš D. MARKOVIĆ<sup>a</sup>, and Saša Ž. ŽIVKOVIĆ<sup>b</sup>**

<sup>a</sup> Faculty of Mechanical Engineering, University of Belgrade, Belgrade, Serbia

<sup>b</sup> Military Technical Institute, Belgrade, Serbia

Original scientific paper

<https://doi.org/10.2298/TSCI200118152J>

*The change of gas parameters in the cylinder of the automatic gun has a great influence on the dynamics of the gun. Many factors have an influence on the gas parameters in the gas cylinder such as the diameter and position of the gas port, the initial volume of the gas cylinder, the gap between the piston and the cylinder, initial temperature of the cylinder parts, etc. The analytical model was made to analyze the parameters on which depends gas piston dynamics. The numerical simulation with CFD software ANSYS Fluent was performed to analyze the change of the thermodynamic properties of the gases in the cylinder, temperature change of the cylinder parts and dynamics of the gas piston. The experiment was performed to provide pressures in the barrel and the gas cylinder and velocity of the gas piston. The comprehensive comparisons between results obtained by the analytical model, the numerical simulation and experiments have been performed and good agreements were observed.*

Key words: *automatic gun, gas cylinder, gas parameters, analytical model, numerical simulation, experimental investigation*

### Introduction

The change of gas parameters in the gas cylinder of the automatic gun has a great influence on the dynamics of the gun. Most of the automatic guns use the energy of the gun powder gases for the drive of the moving parts of the gun. Some of the automatic weapons use a gas piston to control the velocity and position of the breechblock during the entire firing cycle. On the other hand, some automatic weapons use gas piston just for unlocking the breechblock. In both cases it is very important to unlock the breechblock in appropriate time because of two reasons: early unlocking of the breechblock will cause the damage of the cartridge case and late unlocking will effect on the dynamics of the gun. It is necessary to analyze which factors influence the gas parameters changes in time inside the gas cylinder. Some of these factors were analyzed in [1, 2]. Also, the factors on which depends turning of the gas-flow from the barrel into the side orifice were analyzed in [3, 4]. According to a physical process, it was derived the analytical model which describe the dynamic behavior of the piston assembly. The numerical analysis includes transient simulation, dynamic mesh setup using SDOF solver with considering only translational motion along the axis of the cylinder by the analytical model. Due to the com-

\* Corresponding author, e-mail: [djevtic@mas.bg.ac.rs](mailto:djevtic@mas.bg.ac.rs)

plexity of the problem, the numerical simulation was performed in 2-D geometry. To maintain the main properties of the gas-flow, the adaptation of the numerical domain was performed. Boundary and initial conditions for the simulation were defined by the UDF file. To confirm numerical results, the experiment was performed. The experiment provides pressure change in barrel and gas cylinder and they were measured using KISTLER piezoelectric pressure sensors. The dynamic behavior of the gun was recorded with a high speed camera. By recorded videos, it was determined the mean velocity of the piston between two frames. Based on good agreement between numerical and experimental results, the hypothesis can be created that all other thermo-dynamic processes can be analyzed using the numerical simulation.

### Problem description

During the firing process, when the projectile passes by the gas port, fig. 1, combustion gas products enter the gas port and filling up the volume 1. Recirculating zone at the gas port entrance, ie the mass-flow through the gas port depends on the pressure field and the velocity of the gases inside the barrel at the position of the gas port [5]. From volume 1, gases enter volume 2 through the channels 1. After entering into volume 2, gases expand and exert pressure on the piston forehead. The movement of the piston depends on the pressure force that acts on the piston forehead, the force of the piston spring and friction forces that acts on moving parts of the gun that are connected with the piston. Pressure force that acts on the piston forehead depends on the energy of the gases inside the cylinder. During passage through the gas port and channels 1, gases lose energy due to the friction force on the walls and heat transfer caused by forced convection. When entering in to volume 1, gases hit the screw, which represent the stagnation point. In volume 1, gases expand, creating re-circulating zones in volume 1, which also represent energy loss. The passage of the gases through channels 1 and entering volume 2 has the same energy losses as previously explained. The gap between the piston and the cylinder also influences the pressure magnitude in the cylinder. Also, it is necessary to take into consideration the grooves on the outer surface of the piston which produce labyrinth sealing. After unlocking the breechblock, the piston hits the receiver body and stays in that position as long as the pressure force that acts on the piston forehead is higher than the piston spring force. As the pressure in the barrel decreases, the piston goes into the forward position driven by the spring force. In this paper, it will be considered only the period when the piston goes into the rear position (approximately 8 ms) because that period affects the gun dynamics.

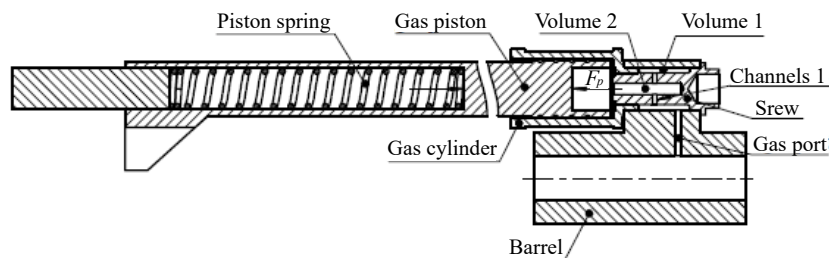


Figure 1. Schematic of the gas cylinder and other parts relevant for the analysis of piston dynamics

### Analytical model

To simplify the analytical model, the flow domain will be divided into the subdomains as shown in fig. 1. Energy loss of the gas-flow will be analyzed in each subdomain and it will

be seen its effect on the pressure in the gas cylinder and the dynamics of the gas piston. The differential equation that describes the motion of the piston can be written in the next form:

$$\left(m_p + \frac{1}{3}m_s\right)\ddot{x} = p(t)A_p - \frac{1}{\varepsilon_s}(F_0 + cx) - F_{fr} \quad (1)$$

Mean pressure change  $p(t)$  in the gas cylinder can be determined based on the First law of thermodynamics for open system:

$$\frac{dp}{dt} = \frac{\kappa - 1}{W} \left[ \dot{m}_{in}h_{in} - \dot{m}_{out}h_{out} - \frac{dQ}{dt} - \frac{\kappa}{\kappa - 1}p \frac{dW}{dt} \right] \quad (2)$$

To study pressure change in the gas cylinder, it is necessary to examine gas-flow through all channels and volumes between the barrel and the cylinder, fig. 1. The flow-through gas port can be studied in two phases. When the ratio between pressures in the gas port and the barrel is less than the critical value, the velocity of the gases and mass-flow at the gas port entrance can be expressed using next equations [6]:

$$V_{in1} = \sqrt{\frac{2\kappa}{\kappa + 1}RT_b} \quad (3)$$

$$\dot{m}_{in1} = C_{D1}A_{in1}\rho_{in1}V_{in1} = C_{D1}A_{in1}\rho_b \left(\frac{2}{\kappa + 1}\right)^{\frac{1}{\kappa - 1}} \sqrt{\frac{2\kappa}{\kappa + 1}RT_b} \quad (4)$$

For the gas port entrance, it is taken the smallest area of the gas port-channel ( $C_{D1}A_{in1}$ ). In the eqs. (3) and (4) it was assumed that the gas-flows isentropically. This assumption is justified since the entrance in the gas port volume is very close to the barrel. As the mean pressure in the gas cylinder increases and the barrel decreases, at some moment, the ratio of the pressures in the gas port and the barrel will reach a critical value. After that moment, the velocity of the gases and the mass-flow at the gas port entrance can be expressed in the next form:

$$V_{in1} = \sqrt{\frac{2\kappa}{\kappa - 1} \frac{p_b}{\rho_b} \left[ 1 - \left(\frac{p_1}{p_b}\right)^{\frac{\kappa - 1}{\kappa}} \right]} \quad (5)$$

$$\dot{m}_{in1} = C_{D1}A_{in1}\rho_{in1}V_{in1} = C_{D1}A_{in1} \frac{p_b}{\sqrt{RT_b}} \sqrt{\frac{2\kappa}{\kappa - 1} \left(\frac{p_1}{p_b}\right)^{\frac{2}{\kappa}} \left[ 1 - \left(\frac{p_1}{p_b}\right)^{\frac{\kappa - 1}{\kappa}} \right]^{\frac{\kappa - 1}{\kappa}}} \quad (6)$$

The inlet enthalpy at the gas port entrance is:

$$h_{in1} = c_p T_{in1} + \frac{1}{2}V_{in1}^2 = c_p T_b \left(\frac{p_b}{p_1}\right)^{\frac{1 - \kappa}{\kappa}} + \frac{1}{2}V_{in1}^2 \quad (7)$$

As it can be seen from eqs. (4) and (6), mass-flow in both flow regimes depends on the re-circulating zone in the gas port entrance. The size of this zone depends on the flow parameters

in the gun barrel and it is taken into account with the discharge coefficient  $C_D$  [5]. The energy loss of the gas-flow in the gas port due to the heat transfer can be expressed in the next form:

$$h[T_g(t) - T_w(t)] + \varepsilon_w \sigma_{SB} [T_g^4(t) - T_w^4(t)] = -\lambda \left. \frac{\partial T_w(r,t)}{\partial r} \right|_{r=R_1} \quad (8)$$

The convective heat transfer coefficient can be expressed in the next form [7]:

$$h = \frac{\lambda_g}{D_h} [3.65 + 0.243 \text{Re}^{0.8} \text{Pr}^{0.4}] \quad (9)$$

$$D_h = \varepsilon d \left( 1 + \varepsilon \frac{d}{d_p} \right) \quad (10)$$

Since the combustion process is not finished when projectile passes by the gas port, there is a possibility that propellant grains enter the gas port. In this paper, it is assumed that propellant grains do not enter in the gas port, so it is taken that hydraulic diameter is equal to the diameter of the gas port. Prandtl number is:

$$\text{Pr} = \frac{\mu_g(T_g) c_p(T_g)}{\lambda_g(T_g)} \quad (11)$$

Using Sutherland's equation, the dynamic viscosity,  $\mu$ , of the combustion gas products can be written in the next form [8]:

$$\mu_g = 1.458 \cdot 10^{-6} \frac{T_g^{1.5}}{T_g + 110.3} \quad (12)$$

The specific heat capacity at constant pressure can be obtained based on thermo-chemical calculations of propellant under standard conditions [9]:

$$c_p = 0.1059 T_g + 1533 \quad (13)$$

Dependence of the thermal conductivity of the combustion gas products on temperature can be written in the next form [10]:

$$\lambda_g = 1.317 \mu_g(T_g) \left[ \frac{3540}{M} + c_p(T_g) \right] \quad (14)$$

After the re-circulation zone, when the streamline is reattached to the gas port wall, a fully developed turbulent flow occurs inside the gas port. Downstream, there is the pressure drop which is caused by friction force. The friction coefficient in the fully developed turbulent flow can be presented with the next equation [11]:

$$\frac{1}{\sqrt{f}} = 2 \log(\text{Re} \sqrt{f}) - 0.8 \quad (15)$$

The enthalpy of the gases at the outlet surface of the gas port (inlet of volume 1, fig. 1) can be calculated based on the difference of the mean pressures in the gas port and volume 1, velocity at the inlet surface, mean temperature of the gases in the gas port taking into account all the losses in the gas port. When the ratio of the pressures is less than the critical value, the

velocity of the gases is equal to the speed of sound. The velocity is evaluated using eq. (3) using the mean temperature at the gas port. The velocity of the gases on the gas port outlet surface, when the ratio of the mean pressures in volume 1 and the gas port is above the critical value, can be determined using the next equation:

$$V_{out1} = \sqrt{\frac{2\kappa}{\kappa-1} \frac{p_1}{\rho_1} \left[ 1 - \left( \frac{p_2}{p_1} \right)^{\frac{\kappa-1}{\kappa}} \right]} + V_{in1}^2 \quad (16)$$

The pressure change in time inside the volume 1 (fig. 2) can be evaluated using eq. (2). The inlet enthalpy is equal to the outlet enthalpy of the gas that comes out from the gas port. In this analytical model, the velocity of the gases around the entrance of the channel 1, fig. 2, is neglected and the discharge coefficient value  $C_{D2}$  may be adopted to be 0.68 according to [5]. The energy losses in volume 1 due to the heat transfer can be calculated using the equations for natural convection [12] (the assumption was made that velocity in volume 1 is small and can be neglected). Also, the gas energy losses in channel 1 are neglected because of the small length and small wall surface area.

For the calculation of the energy loss in the cavity of the screw, the last term in eq. (2) which describes work done by the gases is zero. The dominant mechanism of the heat transfer on the left side of volume 2, fig. 1, is forced convection. On the right side of volume 2, since the fluid is almost at rest, heat is transferred to the walls by conduction and radiation. Gas-flow entering in the gas cylinder (and in the piston forehead cavity), expands and acts on the piston forehead. At the beginning of filling up the gas cylinder, combustion gas products act on the piston forehead with dynamic pressure. Since this dynamic pressure decreases rapidly, it won't be considered in this mathematical model. From the gas cylinder, gases go to the atmosphere through the gap between the piston and the cylinder. More details about the flow through the gap with labyrinth sealing on the piston can be found in [13]. Two re-circulation zones are created in the cylinder, which can be seen in the fig. 9. The velocity of the gases on the gap entrance is relatively small, so it can be assumed that the discharge coefficient at the gap entrance is 0.8 (since there is inflow only from one side). The velocity and the mass-flow at the gap entrance is calculated using eqs. (3)-(6).

### Numerical model

The numerical simulation was performed to investigate the thermodynamic properties of the gases inside the cylinder during the selected period. Based on mass-flow through the inlet boundary of the gun barrel, fig. 1, the flow space of the gas cylinder was modified into the 2-D model based on the 3-D model. The inlet boundary of the barrel was chosen as the referent flow area. After determination of the referent value of the depth, for flow properties calculation in 2-D, it was calculated other dimensions of the flow channels used by Fluent CFD software. The domain of numerical analysis consists of 59300 cells and it is shown in fig. 2. The greater number of the grid cells produce the results that vary approximately 1% and it can be concluded that the grid is optimized. The motion law of the gas piston (translational motion of its center of mass) is defined by the UDF file which is compiled in SDOF solver for dynamic mesh purpose [14]. The initial time for numerical simulation is the moment when the projectile is on the outlet boundary of the numerical domain, fig. 2. The projectile is on the outlet boundary after approximately 1.9 ms. The pressures and temperature changes in time on the inlet (which is defined as pressure-inlet in Fluent) and the outlet boundary (which is defined as pressure-outlet in Fluent)

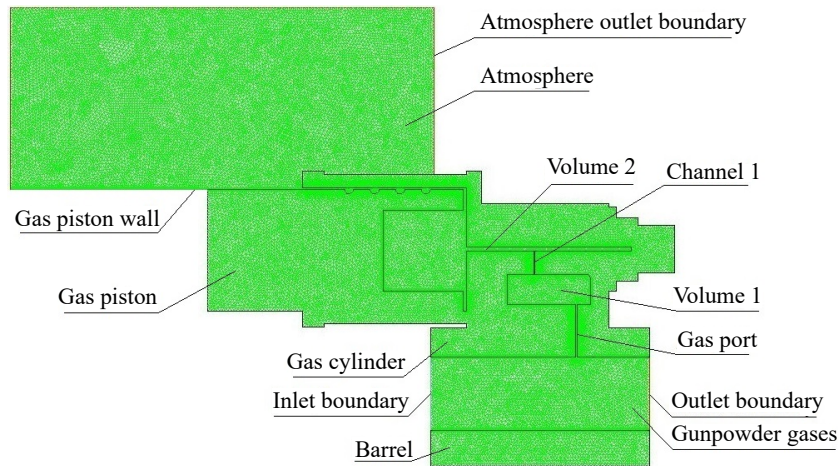


**Figure 2. Numerical domain in CFD ANSYS Fluent with characteristic zones**

of the numerical domain are obtained from interior ballistic calculations [15]. By interior ballistic calculations, it was determined pressure, velocity, temperature, and density of the combustion gas products inside the barrel. The temperature of the surrounding air at the initial time is 300 K. The mechanisms of the heat transfer are convection, radiation, and conduction. The turbulent flow was modeled using RNG  $k-\varepsilon$  model with scalable wall functions. The viscous heating was taken into account. The changes in the physical properties of the gunpowder gases with respect to the temperature are taken into account. The radiation model for the numerical simulation was P-1. More about this model can be found in [16].

### Experimental and numerical results

Experimental results were obtained by firing on proving ground with a 20 mm gun which is shown in fig. 3. Gunpowder gas pressures were measured using KISTLER piezoelectric pressure sensors which were mounted in the barrel at the position of the gas port (KISTLER 6215)

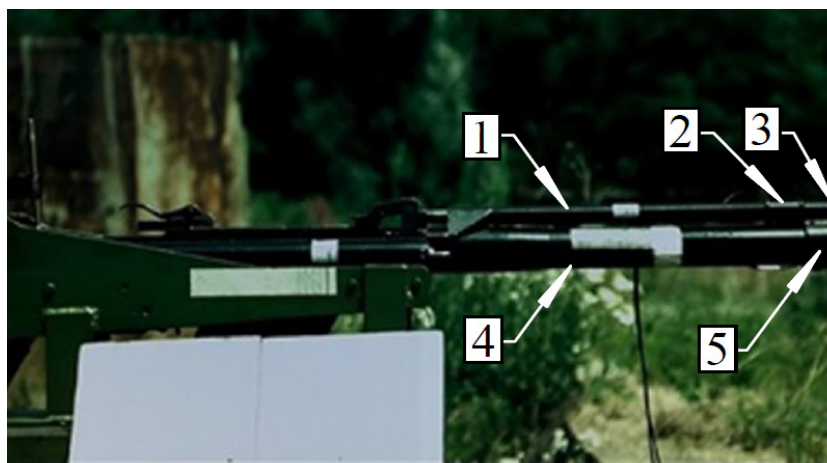


**Figure 3. Experimental investigation-screenshot from high speed camera video of the 20 mm gun; 1 – gas piston, 2 – gas cylinder, 3 – pressure sensor in the gas cylinder, 4 – gun barrel, 5 – pressure sensor in the gun barrel**

and in the gas cylinder (KISTLER 601C) instead of the screw, fig. 1. The velocity of the piston (in the gas cylinder) was determined by recording the gun dynamics with a high-speed camera.

In fig. 4 it is shown pressure distribution in the barrel at the position of the gas port during time obtained by CFD Fluent and experiment. At the initial time for numerical simulation (1.9 ms after the onset of the projectile motion), the difference between experimental and numerical results is approximately 5.5%. After 4 ms it can be seen in the figure that the difference between numerical and experimental results is around 15% which is an acceptable error. In fig. 5 is shown the change of the piston velocity in time. Experimental results of the piston velocity were obtained recording with the high-speed camera, which was set up at 2000 fps. The velocity of the piston was calculated as the mean value between two frames. As can be seen in the figure, all velocities start at the time of  $t = 0$  s. The analytical model and numerical simulation have some delay at the piston movement because of the passage of the gases through all channels. Delay time is not taken into consideration since the start time for the experiment was the beginning of the piston movement.

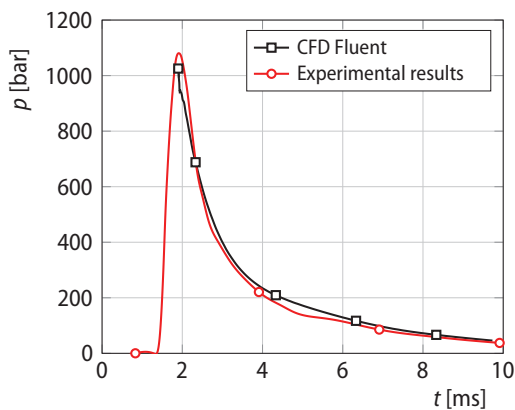


**Figure 4. Gas pressure in the barrel at the position of the gas port-comparison between numerical and experimental results**

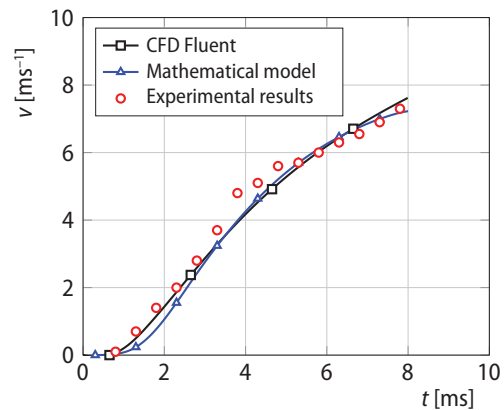


**Figure 5. Piston velocity obtained by analytical, numerical and experimental approach**

The pressure change in the gas cylinder during time is shown in fig. 6. The pressure obtained by the experiment reaches the maximum value of 125 bar after 1.8 ms. The first period of pressure change, shown in the fig. 6 (up to 2 ms), corresponds to the initial phase of slow expansion of the cylinder volume and large mass-flow in the first period. After 1.8 ms the cylinder volume expands at a higher velocity, the density of gunpowder gases decreases in the barrel as well as a velocity of flow at the inlet to the gas port which causes a pressure drop. Figure 6 shows only the pressures obtained by the CFD simulation and experiment because with the analytical model it is possible to obtain only mean value in the cavity of the screw.

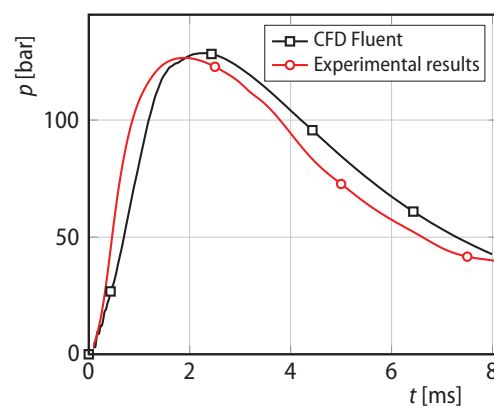


**Figure 6. Pressure in the gas cylinder-comparison of numerical simulation results and experimental data**

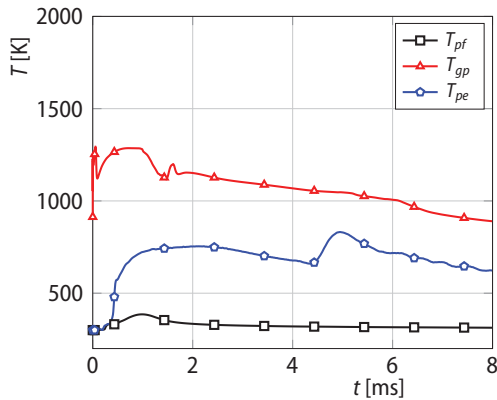


**Figure 7. Temperature distribution in the gas cylinder and piston during time:**

$T_{pe}$  – temperature of the piston edge,  
 $T_{pf}$  – temperature of the piston forehead,  
 $T_{gp}$  – temperature of the piston gas port entrance

forehead is accomplished by forced convection and radiation. The figure shows the change in the temperature of the piston edge which is presented by the blue curve, fig. 7. An increase of temperature up to 830 K can be seen in a time interval of 5 ms. Due to the high flow velocity at the edge of the piston (at the entrance to the gap), a vortex zone occurs. The turbulent flow regime is dominant and causes increased heat transfer. The figure shows the change of the temperature of the gas port at the wall closer to the gun muzzle which is presented by the red curve. The edge of the port represents a stagnation point for gases that flow through the barrel as can be seen in fig. 8. A temperature rise of 1300 K occurs after 0.7 ms. The temperature decrease at the edge of the gas port is caused by the changes of the temperature and velocity of the combustion gas products in the barrel.

In fig. 8 it is shown total temperature distribution around the gas port entrance at the moment of reaching the maximum temperature. On the side of the entrance which is closer to the breechblock, the temperature reaches 1370 K. On this side of the gas port entrance, the re-circulation zone is created in which occurs dominant turbulent flow [17]. In turbulent flow, the heat transfer is enhanced which is the reason for the high temperature of the sidewall in that zone. Downstream along with the gas port, the streamlines are reattached to the wall and the dominant mechanism of the heat transfer is forced convection.

In fig. 9 it is shown velocity field in the piston forehead cavity. Since the velocity of the gases that enter the cavity is high and the piston forehead is relatively close to the gas entrance hole, in the cavity were created two re-circulation zones. These zones influence the heat transfer mechanism in the piston forehead cavity.

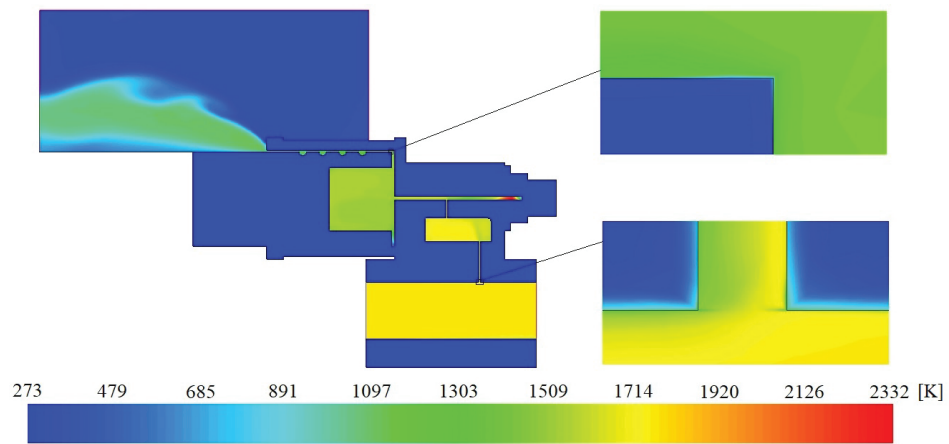
In fig. 10 it can be seen velocity field in the gas port entrance. Dimensions of the re-circulation zone at the entrance influence the velocity and the mass-flow through the gas port and on the dynamics of the piston. That zone depends on the parameters of the flow field in the barrel and on the design parameters of the gas port.

## Conclusion

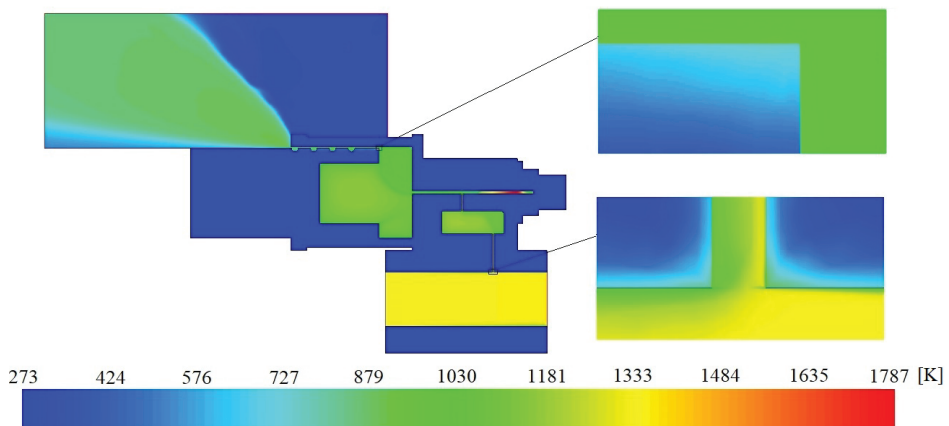
To avoid expensive experiments in the early design phase of the gas cylinder of the automatic weapons, the analytical model was made to observe how to flow field and design

In fig. 7 it is shown temperature distribution during the time in the gas cylinder and the piston. The black curve represents the change in piston forehead temperature. On the figure, it is visible that, the temperature increase of about 100 K and the maximum value occurs after 0.9 ms. The rising temperature is caused by the fact that the piston forehead is a stagnation point for the gases which enter from the screw cavity (volume 2 in fig. 1). After 0.9 ms, the piston forehead surface temperature decrease as a result of the velocity and the temperature decrease of the gases that enter into the gas cylinder. At the same time, the piston is accelerated and the volume of the gas cylinder increases, which causes a drop in the temperature in the cavity of the piston. The mechanism of heat transfer from the gases to the piston

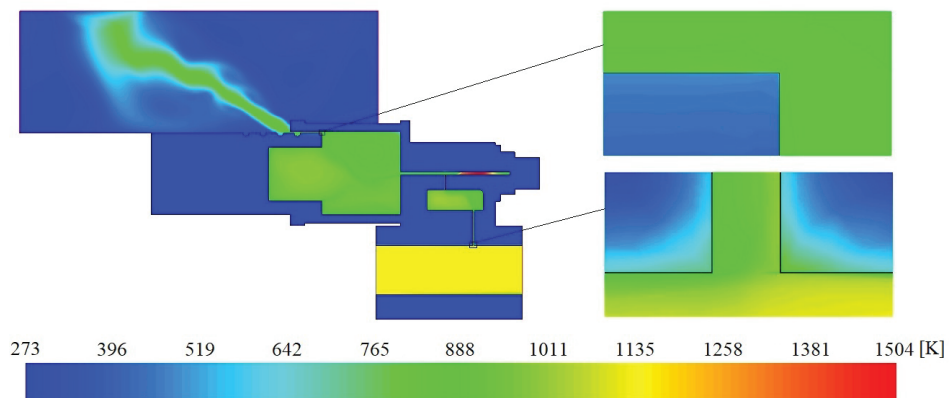




(a)



(b)



(c)

**Figure 8.** Total temperature field in the gas cylinder at the time; (a)  $t = 1$  ms, (b)  $t = 5$  ms, and (c)  $t = 8$  ms

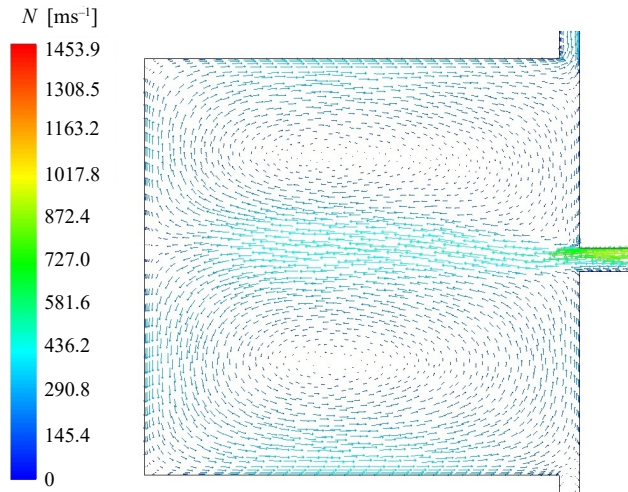


**Figure 9.** Velocity field in the cavity of the piston forehead

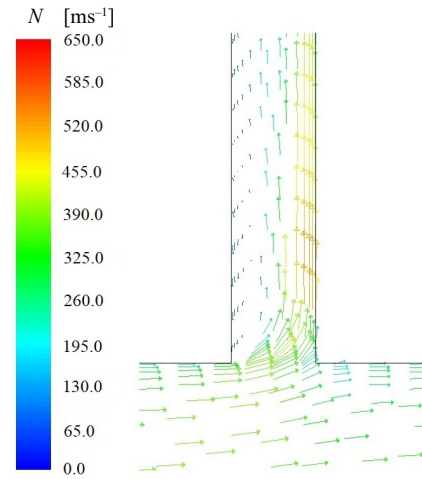


**Figure 10.** Velocity field in the gas port entrance

parameters affect the dynamics of the piston. By the analytical model, it can be calculated the mean values of the pressure and the temperature of the gas in the cylinder. It also can be used for the determination of the piston velocity change in time, which is important for the breechblock unlocking and the total dynamics of the gun. The numerical simulation was performed in 2-D geometry which was modified based on the mass-flow in 3-D geometry. The pressure changes during the time in the gun barrel at the position of the gas port and the gas cylinder were measured with piezoelectric pressure sensors. Based on the good agreement between numerical and experimental results, the assumption was made that all other thermodynamic characteristics of the flow that was obtained numerically correspond to realistic conditions. The numerical simulation provides zones of the gas cylinder and the piston with high temperatures. This is of interest to material selection and surface protection to prevent erosion of the parts of the gas cylinder.

### Nomenclature

$A_{in1}$  – inlet surface area, [m<sup>2</sup>]  
 $A_p$  – piston forehead area, [m<sup>2</sup>]  
 $C_{D1}$  – discharge coefficient, [–]  
 $c_p$  – specific heat capacity at constant pressure, [Jkg<sup>-1</sup>K<sup>-1</sup>]  
 $c$  – spring constant, [Nm<sup>-1</sup>]  
 $D_h$  – hydraulic diameter, [m]  
 $d_p$  – diameter of the gunpowder grain, [m]  
 $d$  – diameter, [m]  
 $F_0$  – initial spring force, [N]  
 $F_{fr}$  – friction force, [N]  
 $h_{in}$  – enthalpy on the inlet surface, [Jkg<sup>-1</sup>]  
 $h_{out}$  – enthalpy on the outlet surface, [Jkg<sup>-1</sup>]  
 $M$  – molar mass of gases, [kgmol<sup>-1</sup>]  
 $m_p$  – piston mass, [kg]  
 $m_s$  – piston spring mass, [kg]  
 $\dot{m}_{in}$  – mass-flow on the inlet surface, [kgs<sup>-1</sup>]  
 $\dot{m}_{out}$  – mass-flow on the outlet surface, [kgs<sup>-1</sup>]  
 $p(t)$  – pressure on the piston forehead, [Pa]

$p_1$  – mean pressure in the gas port, [Pa]  
 $p_b$  – pressure in the barrel, [Pa]  
 $Pr$  – Prandtl number, [–]  
 $Q$  – heat transfer from gases to wall, [J]  
 $R_1$  – inner radius of the gas port, [m]  
 $Re$  – Reynolds number, [–]  
 $R$  – gas constant, [JK<sup>-1</sup>mol<sup>-1</sup>]  
 $r$  – radius, [m]  
 $T_b$  – gas temperature in the barrel, [K]  
 $T_g$  – gas temperature, [K]  
 $T_w$  – wall temperature, [K]  
 $t$  – time, [s]  
 $W$  – volume of the gas cylinder, [m<sup>3</sup>]  
 $x$  – current position of the piston, [m]

### Greek symbols

$\varepsilon_s$  – spring efficiency coefficient, [–]  
 $\varepsilon_w$  – wall emissivity, [–]  
 $\varepsilon$  – porosity, [–]

$\kappa$	– heat capacity ratio, [–]	$\rho$	– density, [ $\text{kgm}^{-3}$ ]
$\lambda_g$	– thermal conductivity of the gas, [ $\text{Wm}^{-1}\text{K}^{-1}$ ]	$\sigma_{SB}$	– Stefan-Boltzmann constant, [ $\text{Wm}^{-2}\text{K}^{-4}$ ]
$\lambda$	– thermal conductivity of the wall, [ $\text{Wm}^{-1}\text{K}^{-1}$ ]		

## References

- [1] X. Han, Y. B., Li, Q., Dynamic Analysis on Gas Operated Device's of Internally-Powered Gatling Weapon, *Proceedings*, International Conference on Electronic and Mechanical Engineering and Information Technology, Harbin, China, 2011, Vol. I, pp. 4661-4664
- [2] Lebedinec, A., *Design and calculation of the gas operated automatic weapons* (in Russian), Moscow State Technical University Bauman, Moscow, Russia, 2006
- [3] Orlov, B., Mazing, G., *Thermodynamic and ballistic basics of solid fuel rocket engine design* (in Russian), Engineering, Moscow, Russia, 1968
- [4] Fansler, K. S., A Simple Method for Predicting Muzzle Brake Effectiveness and Baffle Surface Pressure, Tech. Rep., ARBRL-TR-02335, U. S. Army Aberdeen Research and Development Center, Ballistic Research Laboratories, Aberdeen Proving Ground, Md., USA, 1981
- [5] Sneek, H. J., Witting, P., Bore Evacuator Hole Flows, *Proceedings*, 6. US Army Symposium on Gun Dynamics, Tamiment, Penn., USA, 1990, Vol. I, pp. 61-75
- [6] Korolev, A. A., Komochkov, V. A., *Ballistics of the rocket and barrel weapons* (in Russian), Volgograd State Technical University, Volgograd, Russia, 2010
- [7] Nelson, C. W., Ward, J. R., Calculation of Heat Transfer to the Gun Barrel Wall, Rreport ARBRL-MR-03094, US Army Armament Research and Development Command, Ballistic Research Laboratory, Aberdeen Proving Ground, Md., USA 1981
- [8] Woodley, C., *et al.*, Qinetiq Studies on Wear and Erosion in Gun Barrels, *Proceedings*, RTO AVT Specialists' Meeting on the Control and Reduction of Wear in Military Platforms, Williamsburg, N. Y. USA, 2003
- [9] Micković, D., Jaramaz, S., Tcc – Computer Code for Thermo-Chemical Calculations (in Serbian), Tech. Rep., Weapon Systems Department, Faculty of Mechanical Engineering, Belgrade, 1996
- [10] Jojić, B., *et al.*, *Manual for the Design of Probing Rockets – Volume II Propulsion Group* (in Serbian), SAROJ, Belgrade, 1978
- [11] Munson, B. R., *et al.*, *Fundamentals of Fluid Mechanics*, 7<sup>th</sup> ed., John Wiley and Sons, Inc., New York, USA, 2013
- [12] Cengel, Y. A., *Heat and Mass Transfer-A Practical Approach*, McGraw Hill, New York, USA, 2006
- [13] Kulagin, V., Cerezov, V., *Gasdynamics of the Automatic Weapons* (in Russian), CNII Information, Moscow, Russia, 1985
- [14] ANSYS Inc, 275 Technology Drive Canonsburg, PA 15317, ANSYS Fluent UDF Manual, January, 2015
- [15] Micković, D. M., *Gun Interior Ballistic Cycle Modeling Based on the Two-Phase Flow* (in Serbian), Ph. D. thesis, Faculty of Mechanical Engineering, University of Belgrade, Belgrade, 1999
- [16] Živković, S., *et al.*, Experimental and Simulation Testing of Thermal Loading in the Jet Tabs of a Thrust Vector Control System, *Thermal Science*, 20 (2016), Suppl. 1, pp. S275-S286
- [17] Sherry, M., *et al.*, An Experimental Investigation of the Recirculation Zone Formed Downstream of a Forward Facing Step, *Journal of Wind Engineering and Industrial Aerodynamics*, 98, (2010), 12, pp. 888-894.